Organic/Inorganic Composite Materials: Hydrothermal Syntheses and Structures of the One-, Two-, and Three-Dimensional Copper(II) Sulfate−Organodiamine Phases $[Cu(H_2O)_3(4,4'\text{-bipyridine})(SO_4)]\cdot 2H_2O$, $[Cu(bpe)_2][Cu(bpe)(H_2O)_2(SO_4)_2]\cdot 2H_2O$, and $[Cu(bpe)(H_2O)(SO_4)]$ (bpe = *trans*-1,2-Bis(4-pyridyl)ethylene)

Douglas Hagrman,[†] Robert P. Hammond,[‡] Robert Haushalter,[‡,§] and Jon Zubieta*,[†]

Department of Chemistry, Syracuse University, Syracuse, New York 13244, and NEC Research Institute, 4 Independence Way, Princeton, New Jersey 08540

Received November 17, 1997

Three new members of the copper sulfate/heterocyclic diamine family $[Cu(4,4'\text{-bpy})(H_2O)_3(SO_4)]\cdot 2H_2O$ (**1**; 4,4′-bpy = 4,4′-bipyridine), $[Cu(bpe)_2][Cu(bpe)(H_2O)_2(SO_4)_2]\cdot 2H_2O$ (**2**; bpe = *trans*-1,2-bis(4-pyridyl)ethylene), and $[Cu(bpe)(H_2O)(SO_4)]$ (**3**) have been synthesized using soft chemical methods. Compound **1** crystallizes as light blue needles from the reaction of a mixture of $CuSO_4\cdot 5H_2O$, 4,4′-bipyridine, and H_2O in the mole ratio 1:1:2778, that was heated to 200 °C for 24 h. The structure of **1** consists of linear cationic chains of $\{Cu(4,4'\text{-bpy})(H_2O)_3\}^{2+}$ with SO_4^{2-} anions as spacers between the chains. Compound **2** crystallizes as dark blue rectangular plates from the reaction of a mixture of $CuSO_4\cdot 5H_2O$, bpe, and H_2O in the mole ratio 1:1:1111, that was initially left to stand at room temperature for 24 h and then heated to 120 °C for an additional 24 h. The structure of **2** exhibits rectangular grids constructed from $\{Cu(bpe)_2\}^{2+}$ coordination units with linear $\{Cu(bpe)(H_2O)_2(SO_4)_2\}^{2-}$ chains threaded through the grids. Compound **3** crystallizes as light blue shards from the reaction mixture $CuSO_4\cdot 5H_2O$, bpe, and H_2O in the mole ratio 1:1:1111, that was left at room temperature for 24 h and then heated to 120 °C for 72 h. The structure of **3** consists of one-dimensional $[Cu(bpe)(H_2O)]^{2+}$ cationic chains linked together through the SO_4^{2-} anions to form a three-dimensional framework. Crystal data: $C_{10}H_{18}N_2O_9SCu$ **(1)**: hexaganal $P6_5$, a = 11.2058(2) Å, c = 21.5947(5) Å, V = 2348.35(8) Å, D_{calc} = 1.722 g cm^{-3}; structure determination based on 2255 reflections converged at $R1$ = 0.0488. $C_{18}H_{19}N_3O_6SCu$ **(2)**: monoclinic, $C2/c$, a = 22.9863(1) Å, b = 13.4702(1) Å, c = 13.4902(1) Å, β = 106.030(1)°, V = 4014.71(5), D_{calc} = 1.552 g cm^{-3}; 3504 reflections, $R1$ = 0.0396. $C_{12}H_{12}N_2O_5SCu$ **(3)**: monoclinic Pn, a = 7.851(2) Å, b = 9.9062(3) Å, c = 9.1407(2) Å, β = 98.207(1)°, V = 652.91(3) Å, D_{calc} = 1.850 g cm^{-3}; 1968 reflections, $R1$ = 0.0274.

Introduction

The significant interest in the designed synthesis of solid-state materials reflects their practical applications in areas ranging from heavy construction to microcircuitry. Because organic molecules can alter inorganic microstructures,[1] one approach has focused on the interactive structural hierarchy in organic/inorganic hybrid materials.[2] In such materials, the inorganic moiety contributes to the increased complexity and hence functionality through incorporation as one component in a multilevel structured material where there is a synergistic interaction between organic and inorganic components. This interaction within these hybrid organic−inorganic materials derives from the nature of the interface between the organic component and the inorganic moiety, so synthetic and structural studies of materials exhibiting such an interface will contribute to the development of structure−function relationships for these hybrid materials.

One approach to the design of organic/inorganic hybrid materials employs polytopic ligands to prepare one-, two-, and three-dimensional coordination polymers[3,4] that exhibit electrical conductivity, size and shape selectivity, unusual magnetic properties, and catalysis.[5−8] In the specific case of polytopic organo-

* Corresponding author.
[†] Department of Chemistry.
[‡] NEC Research Institute.
[§] Current address: Symyx Technologies, 420 Oakmead Parkway, Sunnyvale, California 94086.

(1) Stupp, S. I.; Braun, P. V. *Science* **1997**, *277*, 1242.
(2) Smith, J. V. *Chem. Rev.* **1988**, *88*, 148.
(3) Hoskins, B. F.; Robson, R. *J. Am. Chem. Soc.* **1990**, *112*, 1546.
(4) Bowes, C. L.; Ogin, G. A. *Adv. Mater.* **1996**, *8*, 13.
(5) Ermer, O. *Adv. Mater.* **1991**, *3*, 608.
(6) Lehn, J. M. *Angew. Chem. Int. Ed. Engl.* **1988**, *27*, 89.

S0897-4756(97)00756-4 CCC: $15.00
Published on Web 07/21/1998

amine ligands,[9] adamantoid, honeycomb, grid, ladder, railroad, brick wall, and octahedral motifs have been realized using a variety of metal templates.[10−29] The organic spacer serves to tether the metal sites and to propagate the structural information expressed in the metal coordination preferences through the extended structure. This synergistic structural relationship between the metal cation and the organic ligand allows a degree of "crystal engineering" by exploiting fundamental aspects of the coordination chemistry: (i) the identity or oxidation state of the metal and consequently its coordination preferences, (ii) the length of the spacer and the geometry, whether rigid or flexible, and (iii) the relative orientations of the ligand donor groups.

In extending the chemistry of coordination polymers to the preparation of inorganic oxide phases,[30] we noted the dramatic structural influence of the anion on the three-dimensional framework assembly adopted by the coordination polymer cations. Thus, the identity of the anion dictates not only the anion cavity dimensions but the degree of coordination polymer interpenetration and even the polymer framework topology. As part of our continuing investigations of the preparations and structural properties of inorganic oxide−coordination polymer hybrid materials, we sought to examine the role of a simple tetrahedral oxide which would not aggregate into oligomeric structures under the conditions of synthesis and that could potentially act as a bridging ligand between polymer chains. Because Cu(II) readily forms coordination polymers with rigid ditopic organoamines and is also sufficiently oxophilic to coordinate to sulfate anions, the Cu(II)/SO_4^{2-}/organodiamine system was chosen for study. Using 4,4′-bipyridine as ligand, the one-dimensional $[Cu(4,4'\text{-bpy})(H_2O)_3](SO_4)\cdot 2H_2O$ (**1**) was isolated. Upon extending the tether length in *trans*-1,2-bis (4-pyridyl)ethene (bpe), two novel structures are isolated. Compound **2**, $[Cu(bpe)_2][Cu(bpe)(H_2O)_2(SO_4)_2]\cdot 2H_2O$, (**2**) is structurally unique, constructed from interpenetrating square cationic grids of $\{Cu(bpe)_2\}^{2+}$ units, with linear $\{Cu(bpe)(H_2O)_2(SO_4)_2\}^{2-}$ anionic chains filling cavities between the square grids, and linking the grids into a virtual three-dimensional structure. The third compound, $[Cu(bpe)(H_2O)(SO_4)]$ (**3**), is assembled from one-dimensional cationic $\{Cu(bpe)(H_2O)\}^{2+}$ chains connected through SO_4^{2-} anions to form a three-dimensional structure.

Experimental Section

Syntheses were carried out in Parr acid digestion bombs with 23-mL poly(tetrafluoroethylene) liners or in borosilicate tubes with 5/8-in. outside diameter, 3/32-in. wall thickness, and 6-in. length. The $CuSO_4\cdot 5H_2O$, 4,4′-bipyridine (4,4′-bpy), and *trans*-1,2-bis(4-pyridyl)ethylene (bpe) were purchased from Aldrich and used without further purification. Water was distilled above 0.3 MΩ in-house using a Barnstead model 525 Biopure Distilled water center. Infrared (IR) spectra were obtained on a Perkin-Elmer 1600 Series FTIR spectrometer.

Synthesis of $[Cu(4,4'\text{-bipyridyl})(H_2O)_3(SO_4)]\cdot 2H_2O$ (1). A mixture of $CuSO_4\cdot 5H_2O$ (0.050 g, 0.20 mmol), 4,4′-bpy (0.031 g, 0.20 mmol), and H_2O (10 mL, 44% fill volume) in the mole ratio 1:1:2778 was placed in an acid digestion bomb and heated at 200 °C for 24 h. Light blue needles of **1** were isolated in 8% yield based on copper. IR (KBr pellet, cm^{-1}): 3446 (s), 3075 (w), 1606 (s), 1539 (w), 1488 (s), 1412 (m), 1336 (w), 1218 (m), 1108 (vs), 897 (w), 805 (m), 720 (w), 619 (m), 467 (w).

Synthesis of $[Cu(bpe)][Cu(bpe)_2(H_2O)_2(SO_4)_2]\cdot 2H_2O$ (2). A mixture of $CuSO_4\cdot 5H_2O$ (0.05 g, 0.20 mmol), bpe (0.036 g, 0.20 mmol), and H_2O (4 mL, 44% fill volume) in the mole ratio 1:1:1111 was placed in a sealed borosilicate tube and allowed to sit at room temperature for 24 h and then placed in an oven at 120 °C for another 24 h. Dark blue plates were isolated from the bottom of the tube in 23% yield based on copper. IR (KBr pellet, cm^{-1}): 3453 (s), 3077 (w), 1665 (w), 1606 (s), 1506 (w), 1431 (m), 1305 (w), 1255 (w), 1205 (w), 1172 (s), 1121 (w), 1080 (s), 1030 (s), 971 (w), 846 (m), 670 (w), 603 (m), 553 (m) cm^{-1}.

Synthesis of $[Cu(bpe)(H_2O)(SO_4)]$ (3). A mixture of $CuSO_4\cdot 5H_2O$ (0.050 g, 0.02 mmol), bpe (0.036 g, 0.02 mmol), and H_2O (4 mL, 44% fill volume) in the mole ratio 1:1:1111 was placed in a sealed borosilicate tube and allowed to sit at room temperature for 24 h and then placed in an oven at 120 °C for another 72 h. Blue shards were isolated from the tube in 10% yield based on copper. IR (KBr pellet, cm^{-1}): 3455 (s), 3049 (vw), 2374 (vw), 1606 (s), 1505 (w), 1429 (m), 1303 (w), 1176 (s), 1100 (s), 1041 (s), 982 (w), 830 (m), 745 (s), 653 (w), 610 (m), 560 (m), 475 (w).

X-ray Crystallographic Studies. Experimental single-crystal X-ray diffraction data for structures **1**, **2**, and **3** are displayed in Table 1, atomic coordinates with isotropic temperature factors in Tables 2−4, and selected bond lengths and angles are listed in Tables 5−7. Data collection for **1**, **2**, and **3** were performed on a Siemens SMART diffractometer with graphite monochromated Mo Kα radiation [λ (Mo Kα) = 0.71073 Å], equipped with a CCD detector. Data were collected at a temperature of 150 K. Data were corrected for absorption using the psi scan method and corrected for Lorentz and polarization effects. Data processing was accomplished

(7) Frijita, M.; Kwon, Y. J.; Washgzu, S.; Ogwa, K. *J. Am. Chem. Soc.* **1994**, *116*, 1151.
(8) Inoue, K.; Hayamiza, T.; Iwamura, H.; Hashizume, D.; Ohashi, Y. *J. Am. Chem. Soc.* **1996**, *118*, 1803.
(9) Losier, P.; Zaworotho, M. J. *Angew. Chem. Int. Ed. Engl.* **1996**, *35*, 2779.
(10) Batsanov, A. S.; Begley, M. J.; Hubberstey, P.; Stroud, J. *J. Chem. Soc., Dalton Trans.* **1996**, 1947.
(11) Richardson, H. W.; Hatfield, W. E. *J. Am. Chem. Soc.* **1975**, *98*, 835.
(12) Chenggang, C.; Duanjun, X.; Yuanzhi, X.; Chaorong, C. *Acta Crystallogr.* **1992**, *C48*, 1231.
(13) Yaghi, O. M.; Guangming, L. *Angew. Chem., Int. Ed. Engl.* **1995**, *34*, 207.
(14) Santoro, A.; Mighell, A. D.; Reimann, C. W. *Acta Crystallogr., Sect.* B **1970**, *26*, 979.
(15) Hagrman, D.; Zubieta, C.; Rose, D.; Haushalter, R.; Zubieta, J. *Angew. Chem., Int. Ed. Engl.* **1997**, *36*, 873.
(16) Masciocchi, N.; Cairati, P.; Carlucci, L.; Mezza, G.; Gianfranco, C.; Sironi, A. *J. Chem. Soc., Dalton Trans.* **1996**, 2739.
(17) Hagrman, D.; Zapf, P. J.; Zubieta, J., unpublished results.
(18) Blake, A. J.; Hill, S. J.; Hubberstey, P.; Li, W. *J. Chem. Soc., Dalton Trans.* **1997**, 913.
(19) Kawata, S.; Kitagawa, S.; Kondo, M.; Furuchi, I.; Munakata, M. *Angew. Chem., Int. Ed. Engl.* **1994**, *33*, 1759.
(20) Chen, Z. N.; Fu, D. G.; Yu, K. B.; Tang, W. X. *J. Chem. Soc., Dalton Trans.* **1994**, 1917.
(21) MacGillivray, L. R.; Subramanian, S.; Zaworotko, M. J. *J. Chem. Soc., Chem. Commun.* **1994**, 1325.
(22) Yaghi, O. M.; Li, H. *J. Am. Chem. Soc.* **1995**, *117*, 10401.
(23) Otieno, T.; Rettig, S. J.; Thompson, R. C.; Trotter, J. *Inorg. Chem.* **1993**, *32*, 1607.
(24) Hennigar, T. L.; MacQuarrie, D. C.; Losier P.; Rogers R. D.; Zaworotko, M. J. *Angew. Chem., Int. Ed. Engl.* **1997**, *36*, 972.
(25) Robson, R.; Abraham, B. F.; Batten, S. R.; Gable, R. W.; Hoskins, B. F.; Liu, J. *Supramolecular Architecture*; ACS Publication; Washington, D.C., 1992; Chapter 19.
(26) Robinson, F.; Zaworotko, M. J. *J. Chem. Soc., Chem. Commun.* **1995**, 2413.
(27) Carlucci, J.; Ciani, G.; Proserpio, D. M.; Sironi, A. *J. Chem. Soc., Chem. Commun.* **1994**, 2755.
(28) Yaghi, O. M.; Li, H.; Groy, T. L. *Inorg. Chem.* **1997**, *36*, 4292.
(29) Carlucci, L.; Ciani, G.; Proserpio, D. M.; Sironi, A. *J. Chem. Soc. Dalton Trans.* **1997**, 1801.
(30) Hagrman, D.; Zubieta, C.; Rose, D. J.; Zubieta, J.; Haushalter, R. C. *Angew. Chem., Int. Ed. Engl.* **1997**, *36*, 795.

Table 1. Crystallographic Data for $[Cu(4,4'\text{-bpy})(H_2O)_3(SO_4)]\cdot 2H_2O$ (1), $[Cu(bpe)_2][Cu(bpe)(H_2O)_2(SO_4)_2]\cdot 2H_2O$ (2), and $[Cu(bpe)(H_2O)(SO_4)]$ (3)

parameter	1	2	3
empirical formula	$C_{10}H_{18}N_2O_9SCu$	$C_{18}H_{19}N_3O_6SCu$	$C_{12}H_{12}N_2O_5SCu$
crystal system	hexagonal	monoclinic	monoclinic
a, Å	11.2058 (2)	22.9863 (1)	7.2851 (2)
b, Å	11.2058 (2)	13.4707 (1)	9.9062 (3)
c, Å	21.5947 (5)	13.4902 (1)	9.1407 (2)
β, deg		106.030 (1)	98.207 (1)
V, Å^3	2348.35 (8)	4014.71 (5)	652.91 (3)
space group (no.)	$P6_5$ (170)	$C2/c$ (15)	Pn (7)
D_c, g cm^{-3}	1.722	1.552	1.830
$F(000)$	1254	1928	366
Z	6	8	2
FW	405.86	468.96	359.84
μ, cm^{-1}	15.76	12.32	18.56
Mo Kα radiation, Å	0.71073	0.71073	0.71073
2θ min, max, deg	4.20, 50.00	3.54, 50.00	4.12, 56.6
obsd data	2255	3504	1968
no. of parameters	249	298	198
final, *R1*,[a] *wR2*[b]	0.0488, 0.1073	0.0396, 0.0902	0.0274, 0.0733

[a] $R1 = \sum||F_o| - |F_c||/\sum|F_o|$. [b] $wR2 = [\sum w(|F_o| - |F_c|)^2/\sum w|F_o|^2]^{1/2}$.

Table 2. Atomic Coordinates ($\times 10^4$) and Equivalent Isotropic Displacement Parameters (Å$^2 \times 10^3$) for $[Cu(4,4'\text{-bpy})(H_2O)_3(SO_4)]\cdot 2H_2O$ (1)

atom	*x*	*y*	*z*	$U_{(eq)}$
Cu(1)	4274(1)	14(1)	1473(1)	26(1)
S(1)	2321(2)	−3911(2)	1264(1)	28(1)
O(1)	4403(8)	82(9)	2375(4)	33(2)
O(2)	5366(6)	2236(7)	1257(4)	32(2)
O(3)	3807(7)	−616(8)	607(3)	34(2)
O(4)	2625(7)	−3426(6)	619(3)	41(2)
O(5)	837(6)	−4719(7)	1355(3)	54(2)
O(6)	2922(6)	−2703(6)	1678(3)	32(1)
O(7)	2933(8)	−4772(7)	1398(3)	51(2)
O(9)	4762(20)	−3702(16)	2412(10)	72(4)
O(8)	5662(9)	−1195(10)	2919(5)	44(2)
N(1)	2461(6)	39(7)	1527(3)	28(2)
N(2)	6108(6)	39(7)	1422(4)	31(2)
C(1)	1244(9)	−1125(10)	1510(5)	41(2)
C(2)	5(9)	−1159(9)	1487(5)	39(2)
C(3)	−35(8)	56(8)	1477(5)	24(2)
C(4)	1211(9)	1255(9)	1514(9)	38(2)
C(5)	2426(9)	1219(9)	1537(5)	41(2)
C(6)	7316(9)	1197(11)	1433(8)	73(4)
C(7)	8567(10)	1245(10)	1450(8)	68(4)
C(8)	8638(8)	63(8)	1454(5)	28(2)
C(9)	7387(9)	−1132(10)	1419(6)	55(3)
C(10)	6185(10)	−1102(10)	1394(6)	51(3)

Table 3. Atomic Coordinates ($\times 10^4$) and Equivalent Isotropic Displacement Parameters (Å$^2 \times 10^3$) for $[Cu(bpe)_2][Cu(bpe)(H_2O)_2(SO_4)_2]\cdot 2H_2O$ (2)

atom	*x*	*y*	*z*	$U_{(eq)}$
Cu(1)	0	4269(1)	2500	22(1)
Cu(2)	2500	2500	5000	46(1)
S(1)	1228(1)	4630(1)	4344(1)	26(1)
O(1)	879(1)	4236(2)	3313(2)	30(1)
O(2)	893(1)	4394(2)	5112(2)	40(1)
O(3)	1814(1)	4112(2)	4632(2)	39(1)
O(4)	1308(1)	5696(2)	4283(2)	54(1)
O(5)	312(1)	4083(2)	916(2)	41(1)
O(6)	820(2)	2482(2)	−2(3)	72(1)
N(1)	0	5754(2)	2500	28(1)
N(2)	0	2764(2)	2500	28(1)
N(3)	3204(1)	3396(2)	5060(2)	32(1)
N(4)	2419(1)	2343(2)	3455(2)	36(1)
C(1)	444(2)	6271(3)	2726(3)	41(1)
C(2)	−448(3)	7303(3)	2728(3)	68(2)
C(3)	0	7846(4)	2500	59(3)
C(4)	476(2)	2248(2)	2386(2)	39(1)
C(5)	500(3)	1216(3)	2375(3)	60(1)
C(6)	0	650(8)	2500	23(1)
C(7)	220(3)	−410(5)	2471(5)	33(2)
C(8)	212(3)	−1069(5)	2447(6)	36(2)
C(9)	3184(1)	4393(2)	5114(2)	41(1)
C(10)	3670(1)	4985(2)	5084(2)	37(1)
C(11)	4208(1)	4555(2)	5004(2)	25(1)
C(12)	4220(1)	3523(3)	4944(3)	33(1)
C(13)	3719(2)	2982(3)	4970(3)	36(1)
C(14)	4731(1)	5177(2)	5000(2)	27(1)
C(15)	2597(5)	2132(7)	386(8)	26(2)
C(16)	2146(2)	3054(3)	2791(3)	50(1)
C(17)	2165(2)	3069(4)	1768(3)	63(1)
C(18)	2475(2)	2332(4)	1400(3)	62(1)
C(19)	2741(2)	1602(4)	2088(3)	68(1)
C(20)	2707(2)	1625(3)	3091(3)	53(1)

with the SAINT processing program.[31] Direct methods were used to solve all structures using the SHELXTL crystallographic software package.[32] All atoms except hydrogens were refined anisotopically. Neutral atom scattering factors were taken from Cromer and Waber,[33] and anomalous dispersion corrections were taken from those of Creagh and McAuley.[34]

Because there is no mechanism for chiral resolution of **1**, the compound is a mixture of two crystalline forms $P6_5$ and $P6_1$. The crystal used to collect data crystallized in the space group $P6_5$. Absolute configuration was checked by refinement of the 'inverted' and properly translated structure. Compound **2** displays some crystallographic disorder, associated with the ethylene linker of the bpe ligand. This disorder was modeled as equal contributions of two orientations of the bridge.

(31) SHELXTL, Version 5; Siemens Industrial Automation, Inc., 1994.

(32) Software packages SMART and SAINT, Siemens Analytical X-ray Instruments Inc., Madison, WI, 1990.

(33) Cromer, D. T.; Waber, J. T. *International Tables for X-ray Crystallography*; Kynoch; Birmingham, England, 1974; Vol. IV, Table 2.2 A.

(34) Creagh, D. C.; McAuley, J. W. J. *International Tables for X-ray Crystallography*; Kluwer: Boston, MA, 1992; Vol. C, Table 4.2.6.8.

Discussion and Results

Synthesis. Hydrothermal synthesis has been shown to be a valuable method for the preparation of inorganic materials. Bidentate organodiamine ligands that tolerate reaction temperatures in the range 110−260 °C and autogenous pressures can be exploited in effecting crystal engineering. New materials may be isolated by varying the length and rigidity of the bidentate ligand, the identity of the metal center, and the anion incorporated into the solid. As part of our ongoing investigations of the applications of hydrothermal synthesis to

Table 4. Atomic Coordinates ($\times 10^4$) and Equivalent Isotropic Displacement Parameters ($Å^2 \times 10^3$) for $[Cu(bpe)(H_2O)(SO_4)]$ (3)

atom	*x*	*y*	*z*	$U_{(eq)}$
Cu(1)	9199(1)	9772(1)	4663(1)	10(1)
S(1)	7278(1)	11466(1)	2109(1)	11(1)
O(1)	7079(4)	10538(3)	3362(3)	14(1)
O(2)	6670(4)	10748(3)	684(3)	13(1)
O(3)	9248(4)	11816(3)	2155(3)	17(1)
O(4)	6110(4)	12648(3)	2216(3)	19(1)
O(5)	7642(4)	8466(3)	6145(3)	19(1)
N(1)	9375(5)	8216(3)	3217(4)	14(1)
N(2)	9271(4)	1412(3)	−4001(3)	13(1)
C(1)	9297(6)	6937(4)	3687(4)	19(1)
C(2)	9358(6)	5829(4)	2772(4)	19(1)
C(3)	9553(6)	6017(4)	1284(4)	15(1)
C(4)	9698(6)	7349(4)	807(4)	14(1)
C(5)	9602(5)	8407(4)	1789(4)	14(1)
C(6)	9480(7)	4828(4)	309(5)	18(1)
C(7)	9628(7)	4853(4)	−1123(5)	19(1)
C(8)	9491(6)	3656(4)	−2083(4)	15(1)
C(9)	9037(5)	2367(3)	−1625(4)	13(1)
C(10)	8950(5)	1293(4)	−2583(4)	13(1)
C(11)	9711(6)	2640(4)	−4459(4)	17(1)
C(12)	9841(6)	3772(4)	−3549(4)	19(1)

Table 5. Selected Bond Lengths and Angles for $[Cu(4,4'\text{-bpy})(H_2O)(SO_4)]\cdot 2H_2O$ (1)

bond	length, Å	bond	angle, °
Cu(1)—O(1)	1.952(8)	O(1)—Cu(1)—O(2)	100.3(4)
Cu(1)—O(2)	2.207(7)	O(1)—Cu(1)—O(3)	163.8(4)
Cu(1)—O(3)	1.976(7)	O(3)—Cu(1)—O(2)	95.8(3)
Cu(1)—N(1)	2.049(6)	O(1)—Cu(1)—N(1)	89.8(3)
Cu(1)—N(2)	2.044(6)	O(3)—Cu(1)—N(1)	88.4(3)
Cu(1)—O(6)	2.673(6)	O(1)—Cu(1)—N(2)	90.0(3)
		O(3)—Cu(1)—N(2)	92.2(3)
		N(1)—Cu(1)—O(2)	89.5(3)
		N(2)—Cu(1)—O(2)	89.2(3)
		N(2)—Cu(1)—N(1)	178.6(3)
		O(1)—Cu(1)—O(6)	82.4(3)
		N(2)—Cu(1)—O(6)	91.0(2)
		O(2)—Cu(1)—O(6)	177.3(3)
		O(3)—Cu(1)—O(6)	81.5(3)
		N(1)—CU(1)—O(6)	90.3(2)

the preparations of organic/inorganic composite materials, the ligands *trans*-1,2-bis(4-pyridyl)ethylene (bpe) and 4,4′-bipyridyl (4,4′-bpy) were chosen as tethers and spaces between the metal centers. Both ligands were reacted hydrothermally with $CuSO_4\cdot 5H_2O$, to give novel structures consisting of cationic copper organodiamine frameworks with sulfate as the incorporated anion and adopting a variety of coordination modes.

The reaction of $CuSO_4\cdot 5H_2O$, 4,4′-bpy, and H_2O in the mole ratio 1:1:2778 at 200 °C for 24 h yielded a yellow amorphous powder with light blue needles of $[Cu(4,4'\text{-bpy})(H_2O)_3](SO_4)\cdot 2H_2O$ (**1**) in 8% yield. Curiously, the yield of **1** may be significantly improved by introducing MoO_3 into the reaction mixture. However, under these conditions, **1** cocrystallizes with the molybdate phases $[\{Cu(4,4'\text{-bpy})\}_4Mo_8O_{26}]$ and $[\{Cu(4,4'\text{-bpy})_4Mo_{18}O_{47}]\cdot 8H_2O$. Compound **1** is soluble in 2 M sulfuric acid, whereas the molybdate phases are insoluble. In contrast to **2** and **3**, which could be isolated only by hydrothermal techniques, **1** could also be prepared by reacting $CuSO_4\cdot 5H_2O$ and 4,4′-bipyridine in hot water and allowing the resultant solution to cool and stand for several days.

The compound $[Cu(bpe)_2][Cu(bpe)(H_2O)_2(SO_4)_2]\cdot 2H_2O$ (**2**) was synthesized in glass borosilicate tubes by mixing $CuSO_4\cdot 5H_2O$, bpe, and H_2O in the mole ratio 1:1:1111. The tubes are sealed and allowed to sit on the bench top for 24 h, shaken, and placed in the oven for another 24 h. When the glass tubes are removed from the oven and cooled, large dark blue plates are observed in the bottom of the tube in 23% yield. The compound $[Cu(bpe)(H_2O)(SO_4)]$ (**3**) was synthesized by mixing $CuSO_4\cdot 5H_2O$, bpe, and H_2O in the mole ratio 1:1:1111 in a borosilicate glass tube. The tube was allowed to sit on the bench top for 24 h, shaken, and placed in the oven for another 72 h. After the tube was removed from the oven and cooled, **3** was observed as glass-like blue

Table 6. Selected Bond Lengths and Angles for $[Cu(bpe)_2][Cu(bpe)(H_2O)_2(SO_4)_2]\cdot 2H_2O$ (2)

bond	length, Å	bond	angle, °
Cu(1)—O(1)	2.015(2)	N(3)—Cu(2)—O(3)	86.9(1)
Cu(1)—O(5)	2.448(3)	N(3)#2—Cu(2)—O(3)	93.1(1)
Cu(1)—N(1)	2.000(3)	N(4)#2—Cu(2)—O(3)	89.3(1)
Cu(1)—N(2)	2.027(3)	N(4)—Cu(2)—O(3)	90.7(1)
Cu(2)—O(3)	2.649(2)(x2)	N(3)—Cu(2)—N(4)	87.1(1)
Cu(2)—N(3)	2.002(3)(x2)	N(3)—Cu(2)—N(4)#2	92.9(1)
Cu(2)—N(4)	2.052(3)(x2)	N(3)#2—Cu(2)—N(4)#2	87.1(1)
		N(3)#2—Cu(2)—N(4)	92.9(1)
		N(3)—Cu(2)—N(3)#2	180.0
		N(4)#2—Cu(2)—N(4)	180.0
		O(1)—Cu(1)—O(1)#1	177.48
		O(1)—Cu(1)—O(5)	89.0(1)
		O(1)#1—Cu(1)—O(5)	90.8(1)
		O(1)—Cu(1)—N(2)	88.73(6)
		O(1)—Cu(1)—N(2)	88.73(6)
		N(1)—Cu(1)—O(1)	91.27(6)
		N(1)—Cu(1)—O(1)#1	91.27(6)
		O(1)—Cu(1)—O(1)#1	177.5(1)
		N(1)—Cu(1)—O(5)	95.89(7)
		N(2)—Cu(1)—O(5)	84.11(7)
		N(1)—Cu(1)—N(2)	180.00
		O(1)#1—Cu(1)—N(2)	88.73(6)

[a] Symmetry transformations used to generate equivalent atoms: #1, $-x$, y, $-z + 1/2$; #2, $-x + 1/2$, $-y + 1/2$, $-z + 1$; #3, x, $y + 1$, z; #4, $-x$, $y + 1$, $-z + 1/2$; #5, x, $y - 1$, z; #6, $-x + 1$, $-y + 1$, $-z + 1$.

Table 7. Selected Bond Lengths and Angles for $[Cu(bpe)(H_2O)(SO_4)]$ (3)

bond	length, Å	bond	angle, °
Cu(1)—O(1)	1.962(3)	O(1)—Cu(1)—O(2)#1	166.7(1)
Cu(1)—O(2)#1	1.974(3)	O(1)—Cu(1)—N(2)#2	90.3(1)
Cu(1)—N(2)#2	2.029(3)	O(2)#1—Cu(1)—N(2)#2	88.9(1)
Cu(1)—N(1)	2.047(3)	O(1)—Cu(1)—N(1)	90.9(1)
Cu(1)—O(5)	2.288(3)	O(2)#1—Cu(1)—N(1)	88.4(1)
		N(2)#2—Cu(1)—N(1)	173.4(1)
		O(1)—Cu(1)—O(5)	99.4(1)
		O(2)#1—Cu(1)—O(5)	93.9(1)
		N(2)#2—Cu(1)—O(5)	93.9(1)
		N(1)—Cu(1)—O(5)	92.2(1)

[a] Symmetry transformations used to generate equivalent atoms: #1, $x + 1/2$, $-y + 2$, $z + 1/2$; #2, x, $y + 1$, $z + 1$; #3, $x - 1/2$, $-y + 2$, $z - 1/2$; #4, x, $y - 1$, $z - 1$.

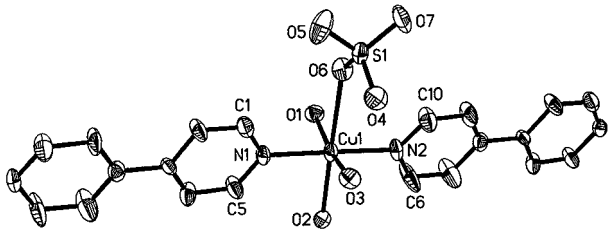

Figure 1. View of the copper coordination geometry in the copper−diamine−sulfate chains of $[Cu(4,4'\text{-bipy})(H_2O)_3(SO_4)]$ (**1**), showing 50% thermal ellipsoids and the atom-labeling scheme.

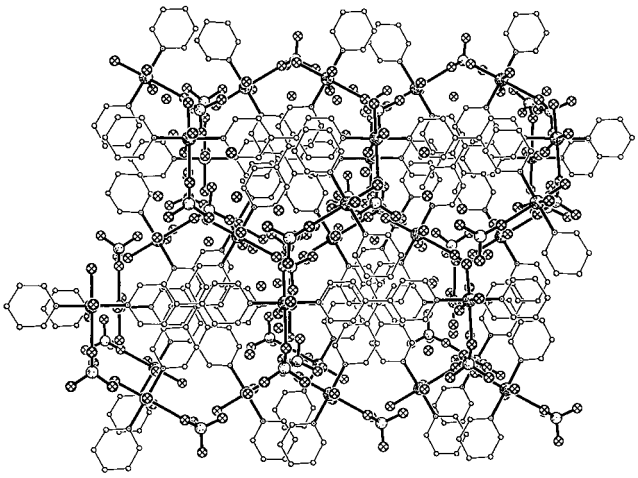

Figure 2. View down the *c*-axis of the stacking of chains in **1** to produce hexagonal cavities accommodating the bpy rings and the H_2O molecules of crystallization.[17]

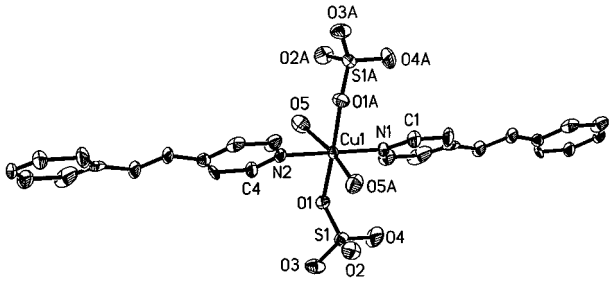

Figure 3. View of the coordination geometry of the Cu(1) sites of **2**, showing the atom-labeling scheme and 50% thermal ellipsoids.

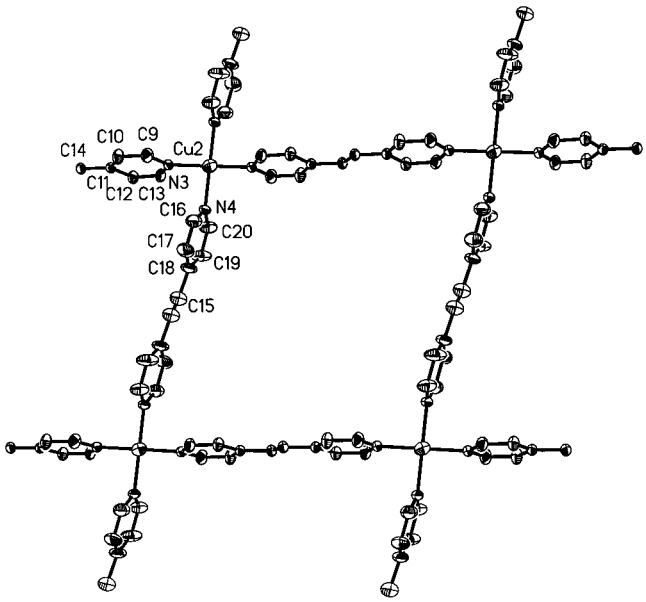

Figure 4. View of the square grids associated with the Cu(2) site of **2**, showing the atom-labeling and 50% thermal ellipsoids.

shards, in the presence of amorphous light blue powder.

Structural Studies. As shown in Figure 1 the structure of **1** is constructed from six coordinate copper sites, exhibiting distorted 5+1 octahedral geometry and linked into linear chains through the 4,4′-bipyridine ligands. The coordination sphere is defined by two pyridyl nitrogen donors from each of two 4,4′-bpy ligands, three aquo oxygen donors, and the oxygen of a sulfate anion. The coordination geometry may be described as a basal plane consisting of the *trans* nitrogen donors N(1) and N(2), with Cu—N distances of 2.049(6) and 2.044(6) Å, respectively, and the aquo ligands associated with O(1) and O(3), with Cu—O distances of 1.952(8) and 1.976(7) Å, respectively. The axial positions are occupied by the aquo ligand O(2) and the oxygen donor O(6) of the sulfate anion. The Cu—O(2) distance of 2.207(7) Å is significantly longer than the equatorial Cu—O distance, whereas the Cu—O(6)

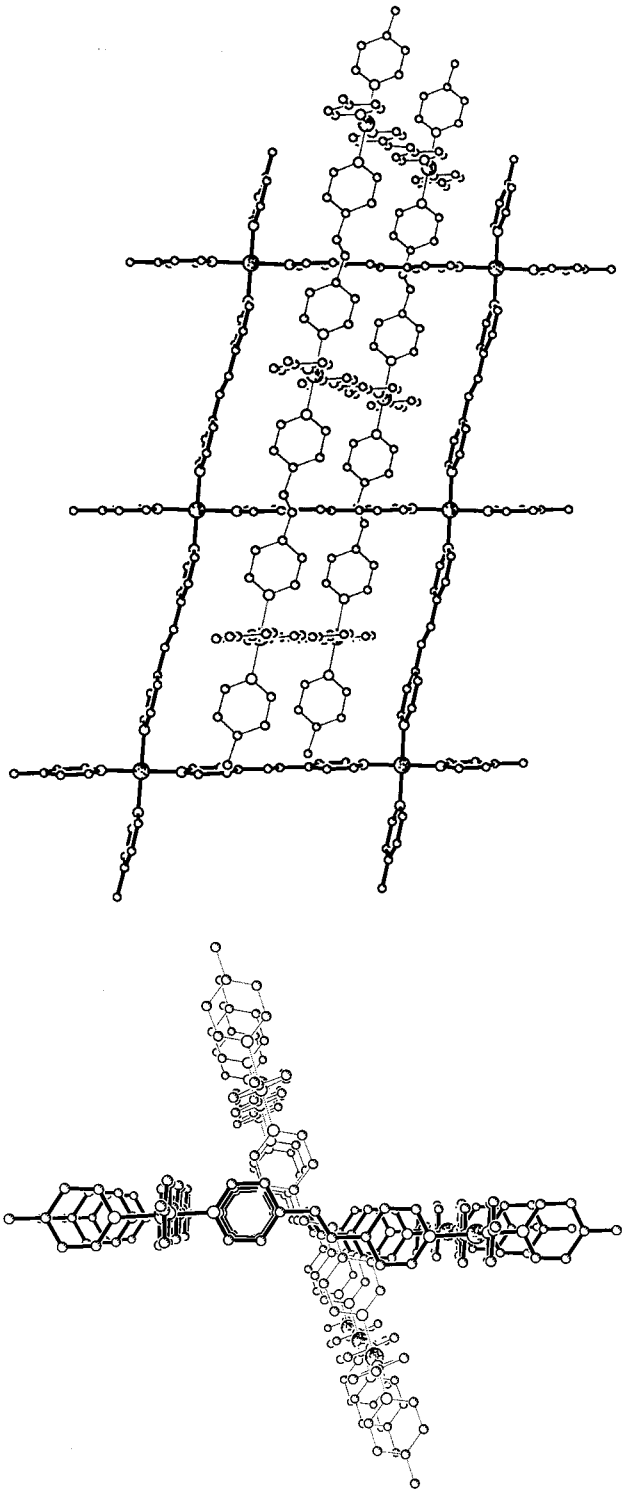

Figure 5. Two views of the interpenetration of square grids in **2**.

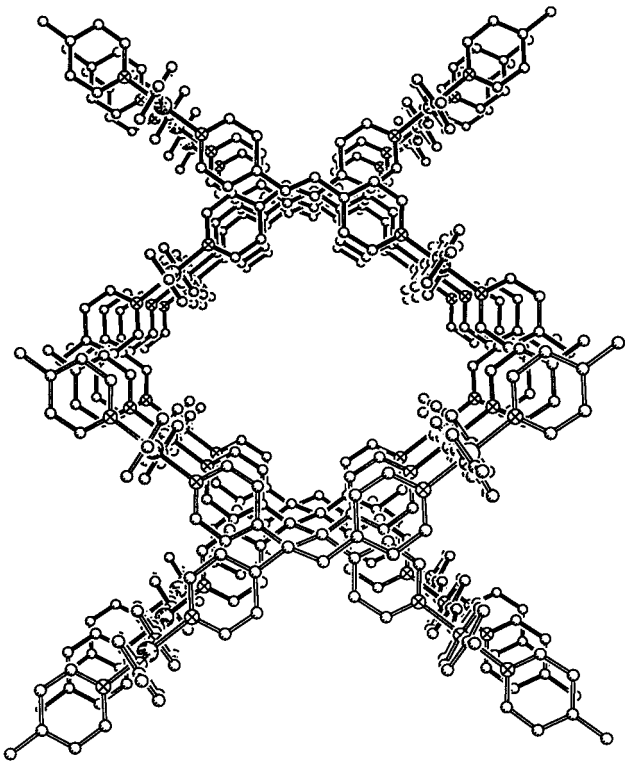

Figure 6. A view parallel to the *c* axis showing the rhombic channels formed by the two sets of interpenetrating square grids.

distance of 2.673(7) Å is indicative of a weak Cu—sulfate interaction.

The $\{Cu(4,4'\text{-bpy})(H_2O)_3\}_n^{2+}$ chains run parallel to the *ab* plane. The weakly coordinated sulfate anions occupy interchain positions and provide the appropriate charge balance. Parallel $\{Cu(4,4'\text{-bpy})(H_2O)_3\}^{2+}$ chains form layers parallel to the *ab* plane and stacking along the *c* axis. Adjacent layers are rotated by 60° to produce virtual hexagonal cavities in projection along the crystallographic *c* axis. The water molecules of crystallization occupy these hexagonal channels (Figure 2).

The structure of $[Cu(bpe)_2][Cu(bpe)(H_2O)_2(SO_4)_2]\cdot 2H_2O$ (**2**) is constructed from two motifs, a linear one-dimensional chain and a two-dimensional grid, which integrate so as to generate a unique three-dimensional framework. As shown in Figure 3, the one-dimensional chains consist of distorted octahedral copper sites bridged by 4,4′-bpe ligands. Each Cu(1) center adopts $\{CuO_4N_2\}$ coordination geometry, defined by two *trans* pyridyl nitrogen donors from each of two bpe ligands, two aquo oxygen donors, and two oxygen donors from two sulfate groups. The six coordination is best described as 4+2 distorted octahedral geometry. The equatorial plane is defined by two pyridyl nitrogen donors with Cu—N distances of 2.000(3) and 2.027(3) Å and two Cu—sulfate oxygen donors at 2.015(2) Å. The axial positions are occupied by aquo ligands with two long Cu—O distances of 2.448(3) Å. In contrast to the structure of **1**, the Cu—sulfate oxygen bonds are proximal whereas the Cu—aquo bonds are distal.

The second structural building block is the two-dimensional square grid pattern adopted by the $\{Cu(bpe)\}^{2+}$ chains of the Cu(2) sites, shown in Figure 4. The proximal coordination at the Cu(2) centers

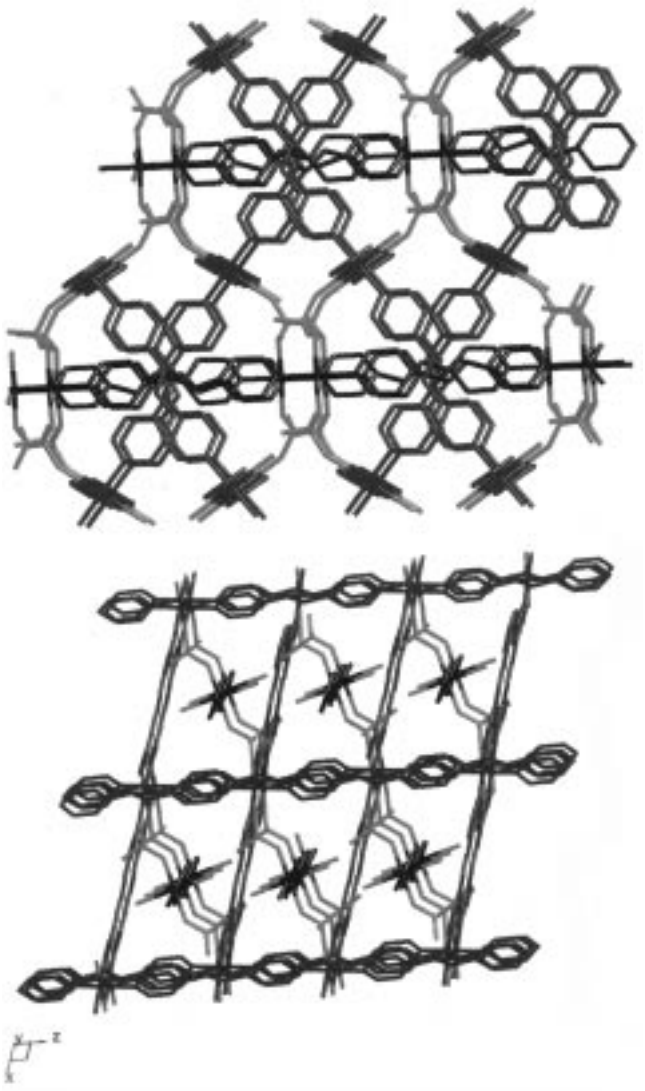

Figure 7. Two stick views of the threading of the one-dimensional $\{Cu(bpe)(SO_4)_2\}_n^{2n-}$ chains through the network of square grids. The square grids are displayed in blue, the one-dimensional chains in black, and the sulfate linkages in orange.

consists of square planar $[CuN_4]$ units, with each Cu(2) bonded to four nitrogen donors from four bpe ligands, producing the grid work pattern of Figure 4. There are two independent sets of parallel gridwork sheets that propagate parallel to the *ab* and *ac* planes so as to interpenetrate at an angle of ~74°, as shown in Figure 5.

When viewed down the *c* axis, the interpenetrating gridwork sheets produce rhombic channels, shown in Figure 6. However, the structure possesses negligible void space because the one-dimensional $\{Cu(bpe)(H_2O)(SO_4)_2\}_n^{2n-}$ chains thread through the square grid networks, as shown in Figure 7. The pyridyl groups and the projecting sulfate arms of the chain nestle snuggly in the cavity formed by the gridwork layers. It is noteworthy that each Cu(2) site of the two-dimensional motifs participates in weak axial coordination to oxygen donors from sulfate groups of two adjacent one-dimensional chains associated with the Cu(1) sites. Consequently, the geometry of the Cu(2) centers is also best described as 4+2 distorted octahedral. The one-dimensional chains are thus linked through weak

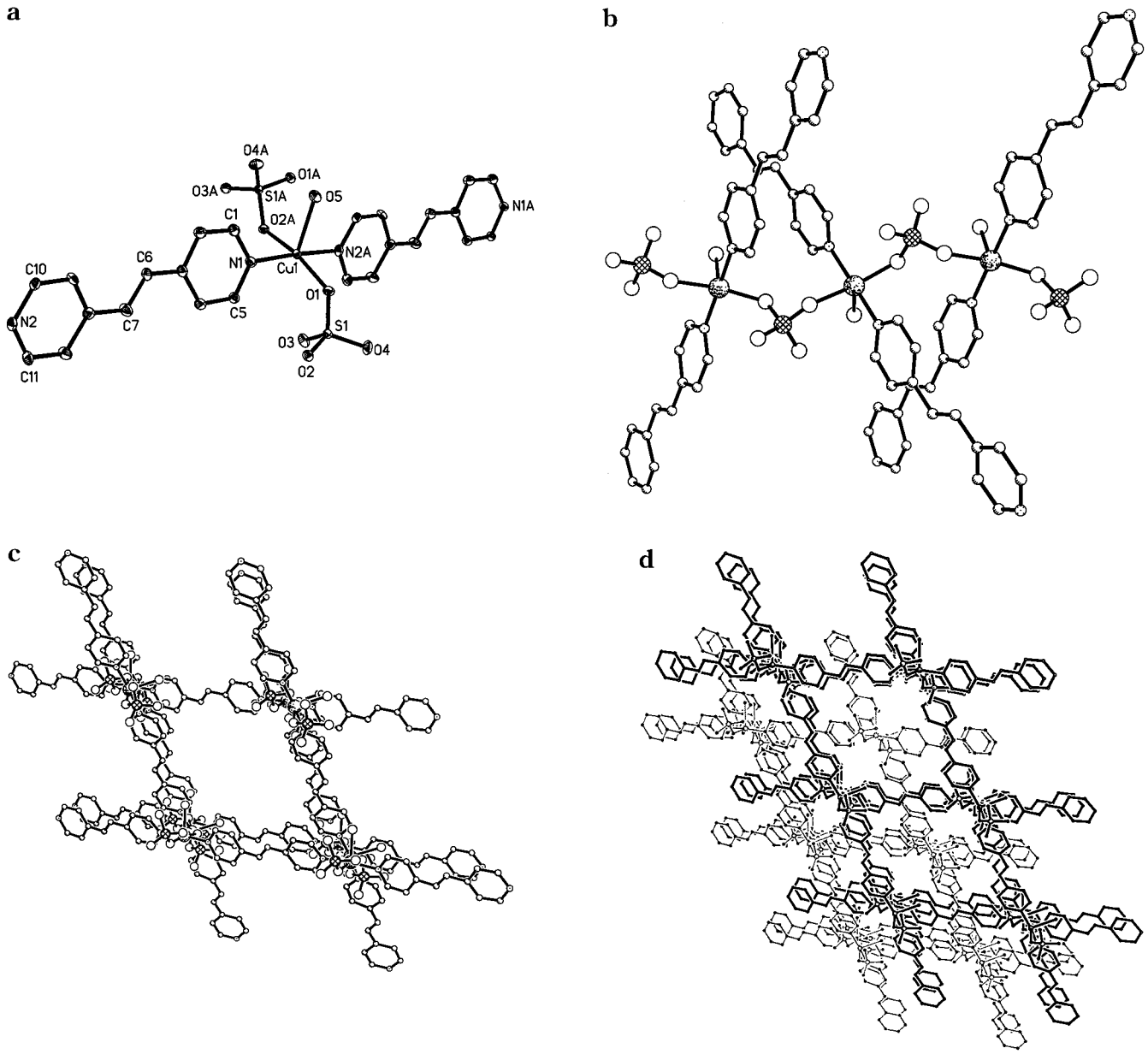

Figure 8. (a) A view of the square pyramidal Cu(II) centers from which the structure of **3** is constructed and showing the atom-labeling scheme and 50% thermal ellipsoids. (b) A view of the $\{Cu(SO_4)\}$ undulating chain that serves to interconnect $\{Cu(bpe)\}_n^{2n-}$ linear chains. (c) A view along the [101] direction showing the resultant rhombic grid. The $\{Cu(SO_4)\}$ chains propagate parallel to the view direction and provide the covalent linkage, which results in the three-dimensional structure of **3**. (d) The interpenetration of the two independent three-dimensional frameworks of **3**.

sulfate bridges to the interpenetrating two-dimensional grids in forming the virtual three-dimersional framework of **2**.

Although the combination of one- and two-dimensional structural motifs is a unique feature of **2**, interpenetration so as to restrict void volume is a common feature of architectures based on coordination polymers.[9] However, open framework structures have been realized by the appropriate selection of anionic constituent,[9] organic guest molecule,[35] or ligand geometry.[36] It would be anticipated that sulfate bridged $\{Cu(bpe)\}^{2+}$ chains could orient to form open framework structures under appropriate conditions. This end was realized by increasing the reaction time of a mixture of $Cu(SO_4)\cdot 5H_2O$ and bpe in water from the 24 h that yielded **2** to 72 h in the preparation of **3**.

The structure of $[Cu(bpe)(H_2O)(SO_4)]$ (**3**) is constructed from one-dimensional chains interlinked through bridging sulfate and 4,4′-bipyridine groups into an open framework, three-dimensional structure. As shown in Figure 8, the chains consist of square pyramidal Cu sites linked throuh bpe ligands. The geometry about the Cu sites is defined by *trans* nitrogen donors from two bpe ligands and two sulfate oxygen groups in the equatorial plane, with an aquo ligand in the axial positon. The Cu—N distances of 2.039(4) and 2.036(3) Å are unexceptional and the Cu—sulfate oxygen distances of 1.972(3) and 1.963(3) Å may be compared with that of 2.016(2) Å for the Cu(1) site of **2**.

(35) Subramanian, S.; Zaworotko, M. J. *Angew. Chem., Int. Ed. Engl.* **1995**, *34*, 2127.
(36) Blake, A. J.; Champress, N. R.; Chung, S. S. M.; Li, W.-S.; Schröder, M. *Chem. Commun.* **1997**, 1005.

The structure propagates in one direction as $\{Cu(bpe)\}^{2+}$ chains through the bridging 1,2-bis(4-pyridyl)-ethylene ligands. These linear chains are linked in turn through bidentate bridging sulfate groups which form a $\{Cu(SO_4)\}_n$ undulating chain (shown in Figure 8b). Adjacent $\{Cu(bpe)\}_n^{2n+}$ chains cross at an angle of ~65° to produce the grid pattern seen in projection along the crystallographic (101) direction, which approximates the direction of propagation of the $\{Cu(SO_4)\}$ chains (Figure 8c). The rhombic channels shown in Figure 8c exhibit a 38-atom connect to generate a cavity of ~5 Å free diameter. Although these microchannels are the dimensions of small pore zeolites,[37,38] there is no significant void space as a consequence of the interpenetration of a second three-dimensional gridwork, as illustrated in Figure 8d. Such interpenetration of independent frameworks is a common feature of such materials and reflects the requirement of efficient packing in the crystalline state.

Compound **3** illustrates the diversity of coordination environments adopted by copper sites in copper-bridging diamine composite solids, for which some structural parameters are presented in Table 8. The table highlights the argument that the structures of such coordination polymers reflect the interplay of the coordination preferences of the metal center, the ligand spacer length and donor group orientation, the properties of the anions, and the presence of neutral guest molecules. The pronounced influence of metal oxidation state is manifest in the contrasting structures of Cu(I) and Cu(II) coordination polymers. The Cu(I) species exhibit predominantly digonal coordination or three coordinate geometries, whereas the Cu(II) species exhibit coordination based on proximal square planar geometry with additional axial interactions, to give the common 4+1 and 4+2 coordination types.

Thermal Behavior. The TGA curves under nitrogen atmosphere for **1**−**3** are shown in Figure 9. The thermal decomposition of **1** is initiated by loss of water in two steps: the first between 40 and 70 °C corresponds to the loss of two water molecules of crystallization, and the second between 80 and 110 °C is attributed to the release of an additional three water molecules. There is a further 41% weight loss in two steps in the 300−400 °C range, which compares with the calculated loss for the 4,4′-bipyridine ligand followed by reduction through release of oxygen. The product of the thermal decomposition of **1** is a black powder that appears to be a mixture of CuS and Cu_2O.

The thermal decomposition of **2** is characterized by a slow dehydration step from 50−170 °C, followed by a weight loss of ~20%, which compares with a calculated value of 19.4% for the loss of one bpe ligand. An additional two ligand molecules are lost over the narrow temperature range 310−315 °C, a process that is accompanied by reduction. The black powdery product is again a mixture of CuS and Cu_2O.

In contrast to the relatively facile dehydration processes of **1** and **2**, **3** exhibits no water loss until 180 °C, whereupon water is lost in a step of 180−230 °C. This water loss is followed by a 53% weight loss from 310 to 400 °C, corresponding to the release of the ligand. Unlike **1** and **2**, which gave black powders as decomposition products, **3** provided a light blue residue that was analyzed for $CuSO_4$.

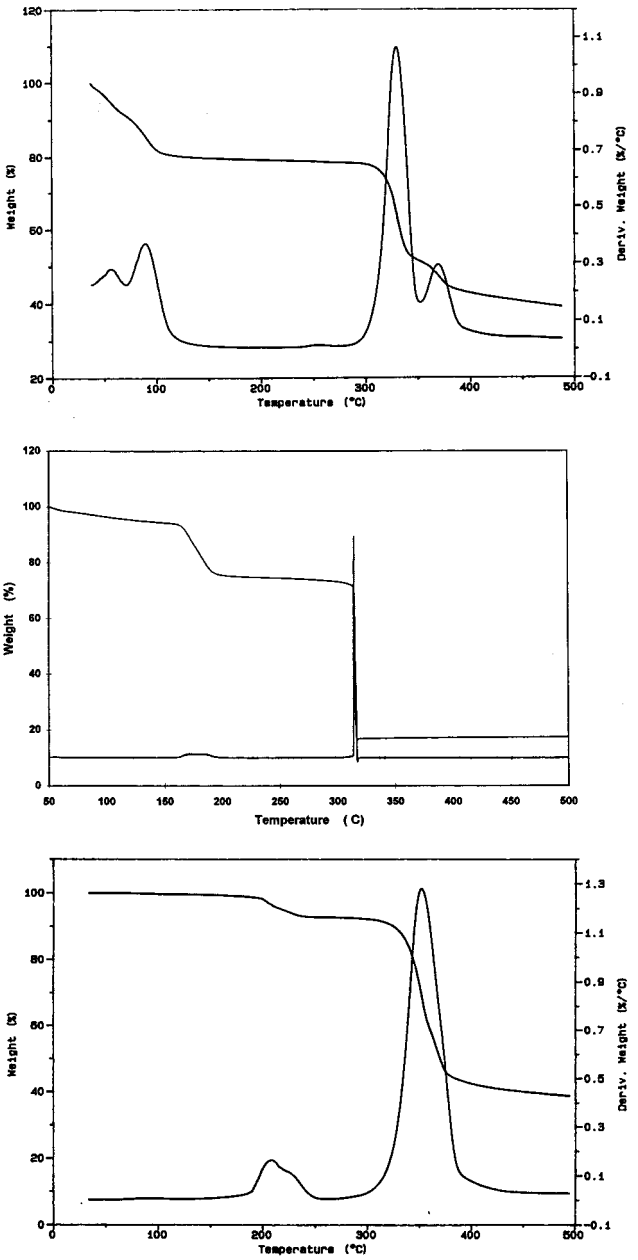

Figure 9. Thermogravimetric curves for the dehydration and thermal decomposition of **1**−**3** (top, middle, and bottom, respectively) under a nitrogen atmosphere.

The dehydration behavior of the materials is not unanticipated. The water molecules of crystallization in **1** and **2** would be expected to be released relatively readily. On the other hand, the coordinated water molecules of **1**−**3** are released at temperatures of 80−110 °C, a range below both 180 and respectively. Because the mechanism of dehydration is dependent on topological and energetic considerations,[39] it should be favored by the accessibility of water molecules to channels present in the crystal structure, as well as to the

(37) Meier, W. M.; Olson, D. H. *Atlas of Zeolite Structure Types*; American Chemical Society: Washington, D.C., 1989.

(38) Ruthven, D. M. *Principles of Adsorption and Absorption Processes*; John Wiley and Sons: New York, 1984.

(39) Petit, S.; Coquerel, G. *Chem. Mater.* **1996**, *8*, 2247.

Table 8. Selected Structural Parameters For Solids of the Copper−Rigid Diamine−Anion Family

compound	Cu oxidation state and coordination	structure	bond distance (Å)	reference
$[Cu(pyr)(NO_3)_2]$	$Cu(II)O_4N_2$	1-D	Cu−O 2.010(4)(x2) 2.490(4)(x2) Cu−N 1.984(4)(x2)	6
$[Cu(C_{10}H_8N_2)(C_{10}H_8N_2)(ClO_4)_2]$	$Cu(II)O_2N_4$	1-D	Cu−O 2.516(7)(x2) Cu−N 1.992(4)(x2) 2.017(4)(x2)	3
$[Cu(4,4'\text{-bpy})(MeCN)_2]BF_4$	$Cu(I)N_4$	1-D	Cu−N 1.961(10) 1.986(10) 2.053(9) 2.090(8)	1
$[\{Cu(4,4'\text{-bpy})\}_4Mo_{15}O_{47}]\cdot 8H_2O$	$Cu(I)N_2$	1-D	Cu−N 1.901(10)(x2)	7
$[Cu(4,4'\text{-bpy})_2(H_2O)_2(BF_4)]$	$Cu(I)O_2N_2$	2-D	Cu−O 1.966(5)(x2) Cu−N 1.983(9) 1.99(1)	10
$[Cu(C_6O_4Cl_2)(C_4H_4N_2)]$	$Cu(II)O_4N_2$	2-D	Cu−O 2.290(2)(x2) 1.955(2)(x2) Cu−N 2.091(2)(2x)	11
$[Cu_2L(4,4'\text{-bpy})_2][ClO_4]_2$ H_2L = *N,N*′-bis(2-aminoethyl)oxamide	$Cu(II)ON_4$	2-D	Cu−O 2.031(3) 1.996(4) 2.041(5) 2.308(4) Cu−N 1.925(4)	12
$[Cu_2L(pym)_2][ClO_4]_2$ H_2L = *N,N*′-bis(2-aminopropyl)oxamide	$Cu(II)ON_4$	2-D	Cu−O 2.019(3) 2.435(5) 2.012(4) 2.026(5) Cu−N 1.925(4)	12
$[CuCl_2(4,4'\text{-bpy})]$	$Cu(II)N_2Cl_4$	2-D	Cu−N 2.075(8) Cu−N 2.128(4) Cu−Cl 2.370(5)(x2) 2.884(7)(x2)	8
$[CuCl_2(4,4'\text{-bpy})]$	$Cu(II)N_2Cl_4$	2-D	Cu−N 2.075(8) 2.128(4) Cu−Cl 2.324(6)(x2) 2.946(6)(x2)	8
$[CuBr_2(4,4'\text{-bpy})]_n$	$Cu(II)N_2Br_4$	2-D	Cu−N 2.075(8) 2.128(4) Cu−Br 2.442(2)(x2) 3.195(3)(x2)	8
$[CuCl(4,4'\text{-bpy})]$	$Cu(I)NCl_3$	2-D	Cu−N 1.995 Cu−Cl 2.433 2.308 2.512	9
$[CuBr(4,4'\text{-bpy})]$	$Cu(I)NBr_3$	2-D	Cu−N 2.020(10) Cu−Br 2.549(2) 2.556(2) 2.463(2)	9
[CuCl(bpe)]	$Cu(I)N_2Cl_3$	2-D	Cu−N 1.999(6) Cu−Cl 2.325(2)(x2) 2.395(2)	9
[CuBr(bpe)]	$Cu(I)NBr_3$	2-D	Cu−N 2.013(8) Cu−Br 2.552(2) 2.470(2)(x2)	9
$[CuCl(4,4'\text{-bpy})]$	$Cu(I)N_2Cl_4$	2-D	Cu−N 1.97(1)(x2) Cu−Cl 2.415(6)(x2) 2.475(6)(x2)	4
$[Cu(4,4'\text{-bpy})_2(PF_6)]$	$Cu(I)N_4$	3-D	Cu−N 2.034(11)(x4)	13
$[Cu_2(pz)_3(SiF_6)]$	$Cu(I)N_4$	3-D	Cu−N not reported	13
$Cu[C_8H_4N]_4BF_4\cdot x\ C_6H_5NO_2$	$Cu(I)N_4$	3-D	Cu−N 2.024(x4)	5
$Cu(4,4'\text{-bpy})_{1.5}\cdot NO_3(H_2O)_{1.5}$	$Cu(I)N_3$	3-D	Cu−N not reported	14
$[Cu(bpe)_2][BF_4]$	$Cu(I)N_4$	3-D	Cu−N 2.003(5) 2.084(6)	37
$[Cu_2(2,5\text{-}me_2pyz)_3][PF_6]_2$	$Cu(I)N_3F_2$	3-D	Cu−N 1.987(4) 1.971(4) 2.085(4) Cu−F 2.69(1) 2.73(3)	15
$[Cu(2,5\text{-}me_2pzy)_2][PF_6]$	$Cu(I)N_4$	3-D	Cu−N 2.126(4)(x2) 2.110(4)(x2)	15
$[\{Cu(4,4'\text{-bpy})\}_4Mo_8O_{26}]$	$Cu(I)O_2N_2$	3-D	Cu−O 2.555(5) 2.691(4) Cu−N 1.915(5) 1.910(5)	7

bonding energy. The relative ease of dehydration of **1** reflects the open one-dimensional structure with hexagonal channels adopted by the material. In contrast, **2** exhibits a complex three-dimensional connectivity based on one- and two-dimensional substructures, there is still considerable void space associated with the rhombic channels produced by the interpenetrating two-dimensional networks. In contrast, the pattern of interpenetration of three-dimensional frameworks in **3** buries the water molecules (Figure 8d) in hydrophobic pockets formed by the aromatic groups of the ligands.

Conclusions

The isolation and characterization of materials **1**−**3** demonstrate the power of hydrothermal techniques in combination with the appropriate choices of organic constituents in effecting the self-assembly of organic−inorganic hybrid materials. It is noteworthy that minor variations in synthetic conditions and tether length in the organic group can result in dramatic structural changes. Although the three materials of this study share as a common structural motif the linear $\{Cu(diamine)\}^{2+}$ chain, the interconnection of chains through the sulfate groups may be expressed in diverse linkages giving rise to unusual structural types. The significant role of the coordinating anions is manifested in the dimensionalities of the phases isolated as well as in the detailed coordination geometry about the copper center. Modifications in tether lengths and the locations of the amine donor atoms and variations of the metal cations and of the anions used in the syntheses appear to permit the exploitation of self-assembly reactions under a variety of synthetic conditions. Most signficantly, sulfate provides a tetrahedral oxide building block that may ligate and bridge metal sites of the coordination polymer chain and hence dictate the interchain geometry and even the dimensionality of the solid. The role of the coordinating anion is clearly manifest in the structure of **3**, which adopts a three-dimensional framework structure with bridging sulfate groups providing the connectivity between $\{Cu(bpe)\}^{2+}$ chains. The vast number of metal−rigid diamine phases reported in the last 2 years is dramatic testimony to the richness of this chemistry and to the significant interest in developing synthetic routes for crystal engineering.

Acknowledgment. This work at Syracuse University was supported by NSF Grant CHE 9617232.

Supporting Information Available: Tables of crystal data, atomic positional parameters, bond lengths and angles, anisotropic temperature factors, and hydrogen atom positions for **1**−**3** (16 pages); crystal structure data for **1**−**3** (19 pages). Ordering information is given on any current masthead page.

CM9707566